JOURNAL OF SOLID STATE CHEMISTRY 15, 140–150 (1975)

Luminescence and Nonradiative Relaxation of Pb^{2+}, Sn^{2+}, Sb^{3+}, and Bi^{3+} in Oxide Glasses*

R. REISFELD AND L. BOEHM

Department of Inorganic and Analytical Chemistry, The Hebrew University of Jerusalem, Israel

AND

B. BARNETT

Soreq Nuclear Research Center, Rehovoth, Israel

Received September 5, 1974

Absorption and fluorescence spectra of Sn^{2+} and Sb^{3+} in borax, phosphate, and germanate glasses were measured in the temperature range 87–295°K. Fluorescence decay times of these ions in borax glass at 87°K was a single exponent with $\tau \approx 6$–11 μsec. At 293°K, two decay times were resolved in the range of 50–2000 nsec. The nonexponential behavior is interpreted by the repopulation of the $^3P_1$ level from the $^3P_0$ level. The temperature dependence of fluorescence and the low values of quantum efficiencies of fluorescence are explained by means of the configurational coordinate diagram model.

Introduction

The optical characteristics of the mercury-like ions, Tl^+, Pb^{2+}, and Bi^{3+} doped glasses were studied recently by Parke and Webb (*1*) and by Reisfeld et al. (*2–4*). As relatively little information on Sn^{2+} and Sb^{3+} is available in the literature (*5*) and these mercury-like ions are important as sensitizers of fluorescence (*6*, *7*), we have made a detailed study of their optical properties in glasses.

A configurational coordinate diagram model is used to explain the low quantum efficiency of mercury-like ions in glasses and the temperature dependence of their spectra.

Experimental

Germanate glasses of the final composition $17K_2O \cdot 17BaO \cdot 66GeO_2$ were obtained from the following materials: GeO_2, Fluka Buchs 99.9%; K_2CO_3, Mallinckrodt; $BaCO_3$, Baker analyzed. For borax glasses the material was Riedel sodium tetraborate, and for phosphate glasses Mallinckrodt $NaH_2PO_4 \cdot H_2O$, 99.5% was used. The dopants Sb_2O_3 and SnO were obtained from B.D.H.

Series of germanate glasses containing Sb_2O_3 or SnO were prepared by mixing the materials mentioned above in an electric vibrator and melting them at 1250°C for 5 h in platinum crucibles. The borax and phosphate glasses were prepared as described previously (*8*). The concentration of Sb_2O_3 and SnO in these glasses ranged between 0.01 and 1.0 wt%.

The absorption spectra measurements were made with a Cary model 17 spectrophotometer against undoped glass as blank. For absorption measurements between 190 and 220 nm, the apparatus was swept by a stream of dry nitrogen. The excitation and emission spectra

* Partially supported by U.S. Army contract DAJA 37-74-C-1628.

were taken on a spectrofluorimeter described previously (*9*). The samples were excited by a 500-W xenon arc lamp or by a deuterium lamp.

The decay times of Sn^{2+}, Sb^{3+}, and Bi^{3+} in borax or phosphate glasses at room temperature were measured using a Nd^{3+} glass laser, excitation by the fourth harmonics (265 nm). [Details for these experiments are given in (*10*).] The decay times of Bi^{3+} and Pb^{2+} in germanate glass at room temperature were measured by a pulse 10 nsec long from nitrogen laser at $\lambda = 337.1$ nm. At 87°K, the decay times of the doped glasses were measured using our spectrofluorimeter, where the light source was replaced by a flash unit with an EGG-FX-6AU flash lamp, having an average pulse duration of 3 μsec.

Results and Discussion

Absorption Spectra

Each of the absorption spectra of 0.01 wt% Sn^{2+} and Sb^{3+} in borax and phosphate glasses at room temperature exhibits one peak. The positions of these peaks for various glasses are given in Table I. In germanate glass the absorption could not be measured directly, because of the high intrinsic absorption of the germanate matrix up to 3000 Å. Therefore, the position of the peak absorption in this glass was estimated by comparing the absorption and excitation of the ions in borax and germanate glasses.

The oscillator strength was calculated by Smakula's formula (*11*):

$$f = 0.82 \times 10^{17} \frac{n}{(n^2+2)^2} \frac{V}{N} \alpha(E)\, dE \quad (1)$$

where n is the refractive index; $(V/N)^{-1}$ is concentrations of ions per cm^3; α is the absorbance in cm^{-1}; and E is the energy in electron volts. The values obtained for Sn^{2+} and Sb^{3+} in borax glass were 0.04 and 0.05, respectively.

Fukuda (*12*) reported the oscillator strengths of Sn^{2+} doped alkali halides at liquid air temperature to be 0.027 for the *A*-band and 0.59 for the *C*-band. Comparing our results with those of Fukuda, we conclude that our recorded peak is the *A*-band, assigned as the $^1S_0 \rightarrow {}^3P_1$ transition.

Excitation Spectra

The excitation spectra of Sn^{2+} and Sb^{3+} in various glasses are presented in Fig. 1. Note that the excitation and absorption maxima do not coincide (due to the spectral properties of the exciting lamp). As previously mentioned, the absorption in germanate glass could not be measured and the data for absorption were calculated as explained in (*4*).

As seen from Fig. 1, the excitation spectra of both Sn^{2+} and Sb^{3+} in borax glass consists of two peaks, the positions of which are given in Table I. Weber (*7*) observed the same phenomenon for Bi^{3+} doped germanate crystals.

TABLE I

SPECTRAL DATA FOR Sn^{2+} AND Sb^{3+} IN VARIOUS GLASSES

	Sn^{2+}				Sb^{3+}			
Matrix	ν_{max} abs. (cm^{-1})	ν_{ex} (cm^{-1})	ν_{emi} (cm^{-1}) main band	Stoke shift (cm^{-1})	ν_{abs} (cm^{-1})	ν_{ex} (cm^{-1})	ν_{emi} (cm^{-1}) main band	Stoke shift (cm^{-1})
Phosphate	44 943	39 215	22 471	22 472	48 190	39 062	21 186	27 006
Borax		39 840				39 370		
	41 322		25 252	16 070	45 410		24 752	23 324
		36 300				36 000		
Germanate	35 211[a]	34 246	24 691	10 520	39 062[a]	33 112	24 390	14 672

[a] Estimated value.

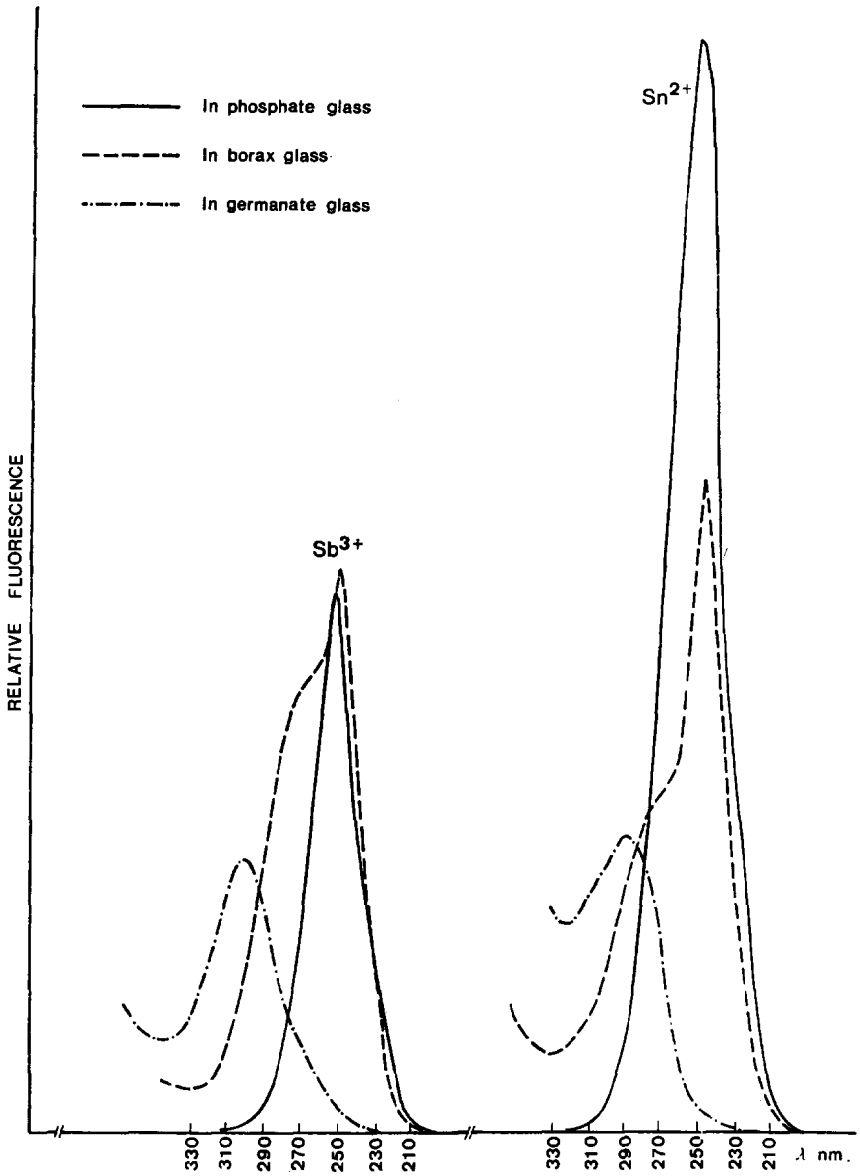

FIG. 1. Excitation spectra of Sn^{2+} and Sb^{3+} in various glasses at room temperature.

He assigned the main excitation band to the $^1S_0 \rightarrow {}^3P_1$ transition and the short wavelength excitation to a single $^1S_0 \rightarrow {}^1P_1$ transition. Since the $^1S_0 \rightarrow {}^1P_1$ transition (the C-band) is an allowed one, it will have an oscillator strength of the order of unity, but this is not the case with our experimental results. As seen from the figure, the heights of the two bands are of the same order of magnitude. Moreover, excitation into both peaks gives the same emission spectra. Therefore, we conclude that the two observed bands are the A_1 and A_2 components of a single A-band assigned to the transition $^1S_0 \rightarrow {}^3P_1$.

A similar explanation was also given by

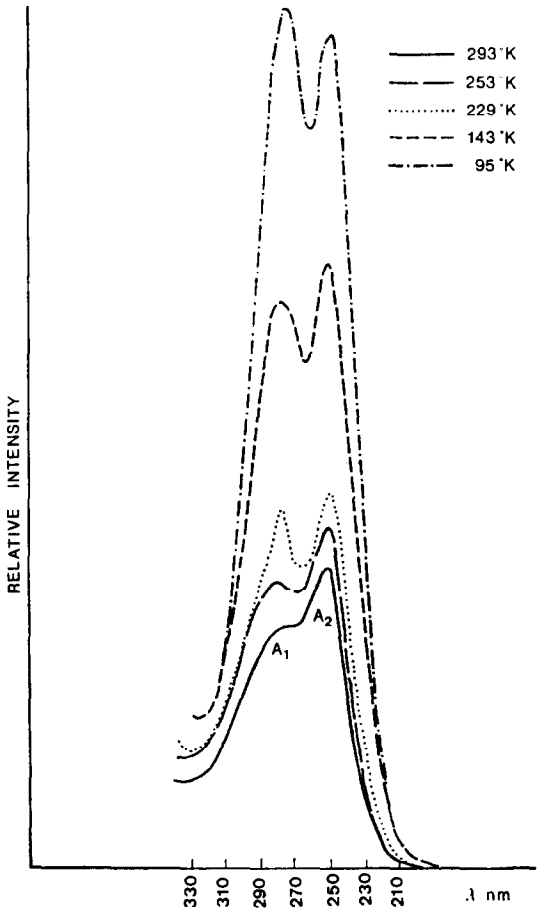

FIG. 2. Temperature variation of the excitation spectra of Sn^{2+} in borax glass.

Fukuda (*12*) for alkali halides doped with s^2 impurities. The splitting of the A-band is due to the Jahn–Teller effect.

The temperature variation of the excitation spectra in borax glass doped with Sn^{2+} is shown in Fig. 2, where a decrease of the total fluorescence with temperature is seen. The same results were obtained for Sb^{3+} The intensity of the A_1-band is lower than that of the A_2-band at room temperature, becomes comparable to the A_2-band at 143°K, and at liquid nitrogen temperature is higher than the A_2-band. The same phenomenon was observed for In^+ doped KCl (*12*).

The inversion of the A_1 and A_2 intensities with temperature could arise from the nonradiative transition rate from A_1 increasing with temperature more rapidly than that of A_2 (*12*). The decrease of the total A intensity is due to temperature enhancement of the nonradiative transitions.

Emission Spectra and Decay Times

The fluorescences of Sn^{2+} and Sb^{3+} arise from the spin forbidden $^3P_1 \rightarrow {}^1S_0$ transition. The emission spectra of Sn^{2+} in various glasses are presented in Fig. 3. A splitting into three bands is observed. The same phenomenon was seen in the emission spectra of Sb^{3+}. The excitation spectra of all the bands is similar, apart from intensity. They might be assigned to emission from the x, y, and z components of the $^3P_1$ state (*13*). This splitting

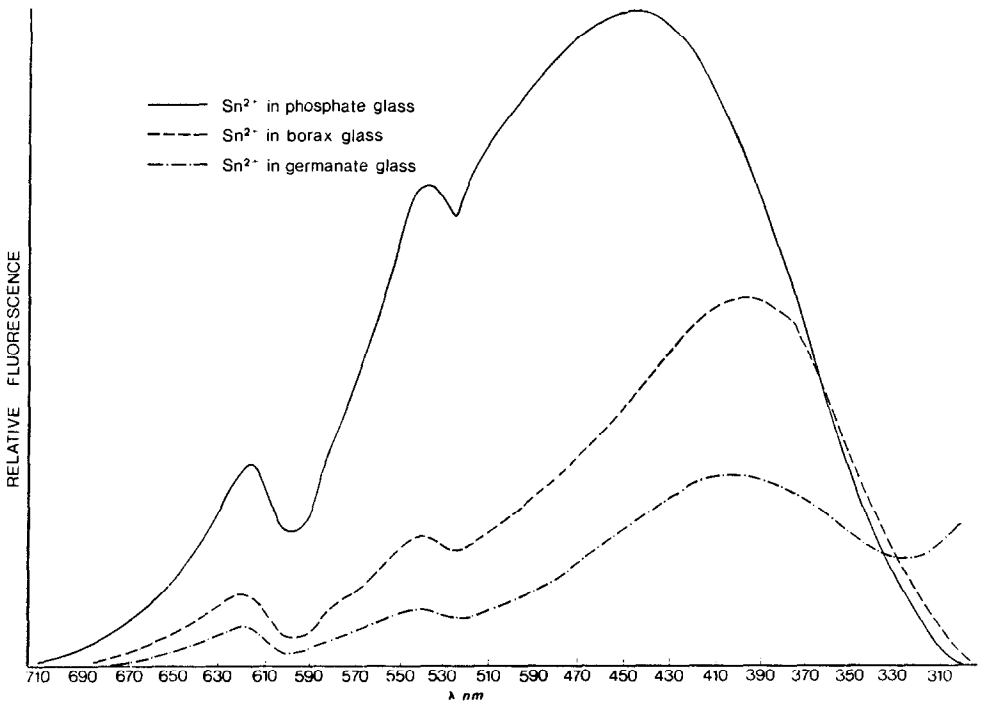

FIG. 3. Emission spectra of Sn^{2+} in various glasses at room temperature.

may arise from the lifting of the $^3P_1$ degeneracy due to the low symmetry of the glass matrix. Such splitting was observed also for crystalline matrices doped by Tl^+ (*14*).

As seen from Fig. 4, thermal quenching of the fluorescence intensity of both Sn^{2+} and Sb^{3+} in borax glass is observed. The results presented in the figure are for the main emission peaks. The variation of the band width of the emission peak with temperature is not significant because it is hidden in the inhomogeneous broadening in the glasses.

A thermal quenching of intensity of fluorescence was observed also for Bi^{3+} doped glasses (*4*). An activation energy was calculated using the Mott and Seitz formula

$$I(0)/I(T) - 1 = C \exp(-\Delta E/kT) \quad (2)$$

where $I(T)$ is the intensity of fluorescence at various temperatures; $I(0)$ is the intensity at 0°K; C is a constant; and k is the Boltzmann constant. The representation of $\log\{[I(0)/I(T)] - 1\}$ as a function of $1/T$ was a straight line. The values obtained for ΔE were 275, 420, and 600 cm^{-1} for Sn^{2+}, Sb^{3+}, and Bi^{3+}, respectively, in borax glasses.

With increases in temperature, the peaks of the main fluorescence band shift to lower energies. The variation of the emission peak position with temperature is more marked in the case of Sb^{3+} than in that of Sn^{2+}, as can be seen from Fig. 5. Other authors (*15*) reported an opposite shift of emission spectra in the case of Sb^{3+} doped calcium halophosphate crystals. However, no explanation was given by these authors.

This phenomenon may be due to nonradiative transitions from one of the high lying $^3P_1$ components to a lower $^3P_1$ component. With increase in temperature, the intensity of the lower component would increase at the expense of the higher component. Since we are unable to resolve the splitting, this would be seen as a shift of the emission peak.

As described in the experimental section,

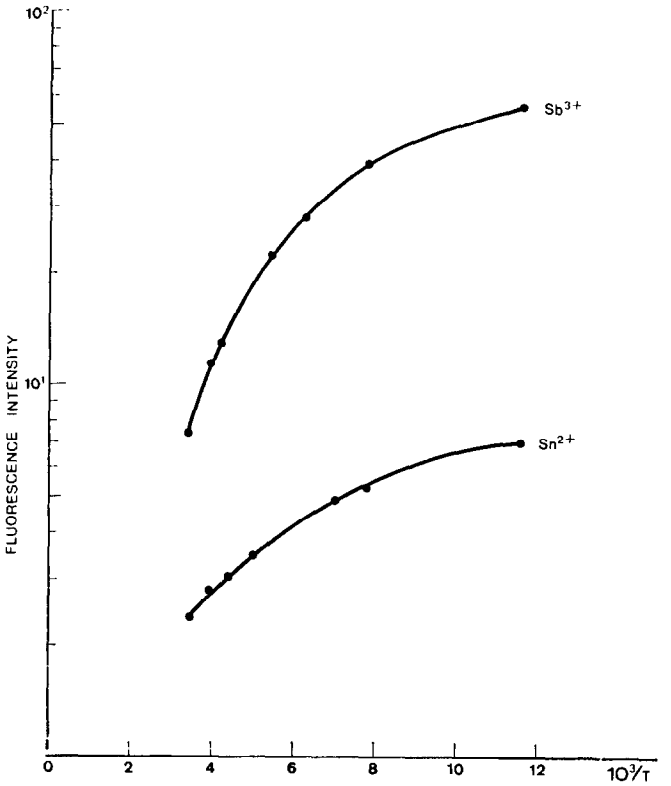

FIG. 4. Temperature dependence of fluorescence intensity of Sn^{2+} and Sb^{3+} in borax glass.

the fluorescent lifetimes of mercury-like ions in glasses at room temperature were measured with a Nd^{3+} glass laser and a Nitrogen laser. The nonexponential decay curves were composed of two decay times, the results of which are given in Table II. In Sn^{2+} and Sb^{3+} doped germanate glass the existing light was absorbed by the matrix resulting in a very low fluorescence; hence, the lifetimes could not be measured.

At 87°K all ions in borax glass exhibited a single lifetime with values given in Table II. These measurements were done with a flash lamp, having an average pulse duration of 3 μsec. The proposed explanation for the existence of two decay lifetimes at room temperatures is as follows. The absorption is from the $^1S_0$ ground state to the $^3P_1$ excited state. The emission occurs also between these levels and is followed by a Stokes shift. Part of the population of the $^3P_1$ is rapidly depleted by a radiationless process to the metastable $^3P_0$ state (Fig. 6), giving rise to the observed fast decay component. At room temperature, thermal equilibrium is established between the $^3P_1$ and $^3P_0$ population, giving rise to an emission rate that is the thermally weighted average of the emission rate of the two states, resulting in the long decay component observed from the $^3P_1$ level. The rate of thermalization is the rate of back transfer from the $^3P_0$ to $^3P_1$ level, which controls the population of the $^3P_1$ level. Since both the short lifetime emission and the delayed emission were observed at the same wavelength, we conclude that the two decay times are due to emission from the same level. Similar phenomena were also observed for other mercury-like ions in glasses (*4*, *16*).

The fact that more than one process occurs during the decay of the $^3P_1$ state also explains the deviation of the decay curve at room temp-

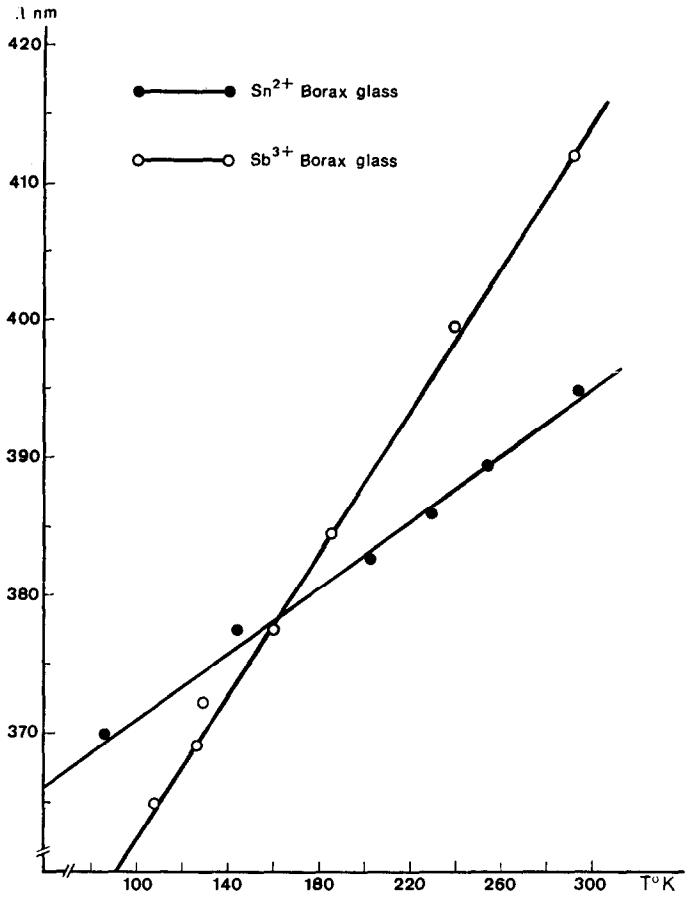

FIG. 5. Variation with temperature of the emission peak position of Sn^{2+} and Sb^{3+} doped borax glass.

TABLE II

DECAY TIMES OF MERCURY-LIKE IONS IN VARIOUS GLASSES[a]

Matrix	Sn^{2+} (nsec)	Sb^{3+} (nsec)	Pb^{2+} (nsec)	Bi^{3+} (nsec)
Phosphate	—	$67.2^{(r)}$, $2000^{(r)}$	—	—
Borax	$11\,300^{(l.a.)}$	$92.8^{(r)}$, $2300^{(r)}$ $6500^{(l.a.)}$	—	$25^{(r)}$, $333^{(r)}$ $19\,000^{(l.a.)}$
Germanate	—	—	$29^{(r)}$, $260^{(r)}$	$37^{(r)}$, $350^{(r)}$ $17\,000^{(l.a.)}$

[a] (r) = room temperature; $(l.a.)$ = liquid air temperature.

erature from a simple exponential. At liquid air temperature, the tunneling from $^3P_0$ to $^3P_1$ is very slow and this is reflected in the long component of lifetime, which is longer by two orders of magnitude than at room temperature.

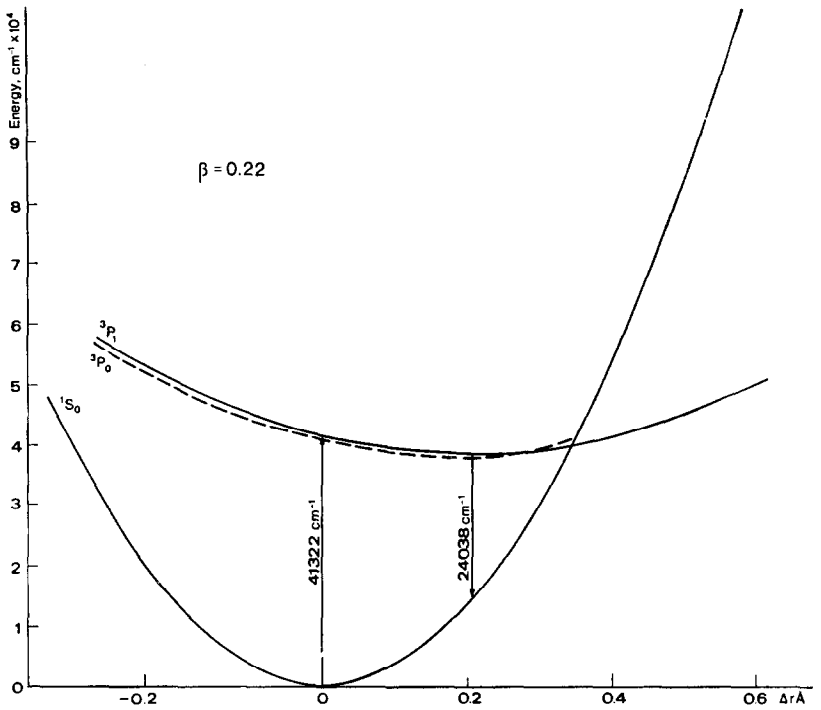

FIG. 6. Configurational coordinate diagram for Bi^{3+} in borax glass.

Quantum Efficiencies

As explained in detail in (*4*), the *Q.E.* of mercury-like ions can be determined by the comparative method using the formula:

$$Q_u = Q_s[A_u D_s \lambda_s n_u^2 / A_s D_u \lambda_u n_s^2] \quad (3)$$

where Q is the quantum efficiency; A is the corrected emission peak area; D is the optical density at the excitation wavelength λ; n is the refractive index; and subscripts s and u denote standard and unknown, respectively.

The comparative method could not be applied in the usual way in the case of mercury-like ion doped glasses because of the high self-absorption of the glasses at the excitation wavelength. Therefore, determination was made by comparing the emission intensity of 0.5 wt% Sn^{2+} or Sb^{3+} in phosphate, borax, and germanate glasses to 0.5 wt% Tl^+ doped borax glass, using the fact that at this concentration the exciting light was totally absorbed in all glasses and the light flux on the measured glass and the standard glass was equal. The *Q.E.* of the standard Tl^+ doped borax glass was found to be 18.7 ± 1.5% (*16*).

The *Q.E.* obtained at room temperature for Sn^{2+} and Sb^{3+} are given in Table III.

TABLE III

PERCENTAGE OF QUANTUM YIELDS (*Q.E.*) OF Sn^{2+}, Sb^{3+}, Pb^{2+}, AND Bi^{3+} IN VARIOUS GLASSES

Matrix	Sn^{2+}	Sb^{3+}	Pb^{2+} (3)	Bi^{3+} (4)
Phosphate	3.6 ± 0.5	0.065 ± 0.01	—	0.003 ± 0.001
Borax	1.6 ± 0.4	0.043 ± 0.01	1.0 ± 0.5	0.14 ± 0.2
Germanate	0.01 ± 0.002	0.024 ± 0.005	4.4 ± 1.4	1.9 ± 0.3

They are compared to those of Pb^{2+} and Bi^{3+} doped glasses (*4*). As seen from the table, the quantum efficiency of Bi^{3+} increases from phosphate to germanate glass but an opposite behavior is seen in the case of Sn^{2+} and Sb^{3+}. This is due to high absorption of the germanate host matrix at the excitation wavelength of Sn^{2+} and Sb^{3+} and the absence of energy transfer from the host to those dopant ions.

Configurational Coordinate Diagrams

A two-state configurational coordinate diagram in which the upper $^3P_1$ and lower $^1S_0$ states have the same force constants was used by Parke and Webb (*1*) in their interpretation of the fluorescence of Tl^+, Pb^{2+}, and Bi^{3+} in glasses. This assumption, however, is not consistent with the observed quantum efficiencies and fluorescence temperature dependence, since it leads to a barrier height (height of the crossing point of the curves above the $^3P_1$ minimum) of about 16 000 cm^{-1}, when taking the positions of the absorption and emission peaks into consideration. The experimental results lead to an activation energy of about 600 cm^{-1} (for example, Bi^{3+} in borax glass). A more realistic model is one in which the $^3P_1$ potential force constant is lower than that of the $^1S_0$.

Note, however, that three emission peaks are observed originating from the $^3P_1$ state (Fig. 3). They arise from the lifting of the threefold degeneracy of the $^3P_1$ state due to the low symmetry of glasses [the C_s symmetry (*16*)]. In the fluorescence experiments, we observed that while the total emission decreases with temperature, the relative emission intensity of each component is temperature independent. For this reason, in the following discussion we may restrict ourselves to an analysis of the most intense emission peak occurring at the highest energy. The emission intensity of this peak is about 10 times that of the other two.

We have calculated the barrier height as a function of the ratio of the force constants β of the $^3P_1$ and $^1S_0$ states. The results are presented in Table IV and the detailed derivation appears in the Appendix.

In borax glass the energy of the electronic ground-state phonon is given by the B–O stretching frequency, i.e., 1400 cm^{-1} (*4*). To see an activation energy in the emission from the $^3P_1$ state of Bi^{3+}, it is necessary that the nonradiative transition rate change drastically on going from the lowest vibronic level of the excited electronic state to the next vibronic level (*17*). Under these circumstances the upper state phonon energy $\hbar\omega_u$ should be of the order of the activation energy. Within the experimental error, the latter is 600–700 cm^{-1}. To obtain a value of $\hbar\omega_u \sim 660$ cm^{-1} the value of β should be 0.22. Note that for Tl^+ doped KCl (isoelectronic with Bi^{3+}), the force constant ratio is about 0.4 (*18*).

From the position of the experimental absorption and emission peaks, and the estimated value of β, we are able to draw the configurational coordinate diagram for mer-

TABLE IV

BARRIER HEIGHT AS A FUNCTION OF THE FORCE CONSTANT β[a]

β	Coordinate shift $2B$ (Å)	Energy difference $2A$ (cm^{-1})	Barrier height H (cm^{-1})
0.02	0.226	40 983.6	105.0
0.04	0.224	40 657.4	214.2
0.06	0.222	40 343.8	329.0
0.08	0.220	40 041.4	446.6
0.10	0.218	39 750.2	569.8
0.12	0.216	39 470.2	697.2
0.14	0.214	39 200.0	828.8
0.16	0.212	38 938.2	966.0
0.18	0.210	38 684.8	1107.4
0.20	0.209	38 441.2	1255.8
0.21	0.208	38 322.2	1331.4
0.22	0.207	38 204.6	1408.4
0.23	0.206	38 089.8	1486.8
0.24	0.205	37 976.4	1566.6
0.26	0.204	37 755.2	1730.4
0.28	0.202	37 541.0	1901.2
0.30	0.200	37 333.8	2077.6
0.32	0.199	37 132.2	2261.0
0.34	0.197	36 936.2	2450.0
0.36	0.196	36 747.2	2647.4
0.38	0.195	36 562.4	2850.4
0.40	0.193	36 383.2	3061.8

[a] Absorption, 41 322 cm^{-1}; emission 24 038 cm^{-1}; $\hbar w$, 1400 cm^{-1}.

cury-like ions in glasses. In Fig. 6, we present the C–C curves for Bi^{3+} in borax glass. In this figure, we have only drawn those C–C curves relating to the $^1S_0$ and most intense $^3P_1$ component. The position of the $^3P_0$ level is not known, but is drawn in approximately by a dashed curve.

The low quantum efficiency of the ions Sn^{2+}, Sb^{3+}, Pb^{2+}, and Bi^{3+} in glasses is due to the excitation being above the $^1S_0$–$^3P_1$ crossing point, as calculated in this work. Note here that if the force constants were equal, the excitation would be below the crossing points, making it difficult to account for the low value of the quantum efficiency.

Appendix

To obtain a semiquantitive picture of the physical events and estimation of the ratio of the force constants and other parameters of the C–C curves, we present a C–C model based on several simplifying assumptions that will be stated in the text as they arise.

The potential occurring in the C–C diagram may be expresssed as follows:

$$V_u = (\beta/2)\,[(Q-b)^2 + a] \qquad (|p\rangle \text{ potential well}) \quad (2a)$$

$$V_g = (1/2)\,[(Q+b)^2 - a] \qquad (|s\rangle \text{ potential well}) \quad (2b)$$

where $2a$ is the energy difference between the minimum of the upper and lower potential curves (in units of $\hbar\omega_g$, the frequency of the lower potential well) $2b$ is the coordinate shift of the upper C–C relative to the lower, Q is the nuclear displacement, both in units of $\sqrt{(\hbar/mw_g)^{1/2}}$, the zero point motion in the ground state, and β is the ratio of the upper force constant (K_u) to the lower force constant (K_g).

$$\beta = K_u/K_g = m_u(\hbar w_u)^2/[m_g(\hbar w_g)] \quad (3a)$$

resulting in

$$\beta = \hbar w_u/\hbar w_g)^2 \qquad (\text{when } m_u \approx m_g). \quad (3b)$$

For a given value of β, parameters a and b may be obtained from the position of the experimental absorption peak (E_{abs}) and emission peak (E_{emis}):

$$E_{abs} = 2a + 2b^2\beta \quad (4a)$$

$$E_{emis} = 2a - 2b^2. \quad (4b)$$

The barrier height H as a function of β is given by

$$H = \frac{1}{2}\beta\{-b + \frac{1}{2}\left[\frac{b + \beta b \pm (4a - 4\beta a + 4\beta b^2)^{1/2}}{(\beta/2) - (1/2)}\right]^2\}. \quad (5)$$

In formula (5) we have taken the lowest of the two crossing points when calculating the barrier height. Quantities a and b are completely determined by E_{abs}, E_{emis}, and the value of β.

Acknowledgment

The authors are grateful to Dr. Sh. Goldschmidt for performing the lifetime measurements with the Nd^{3+} glass laser.

Note. Recently the first author had a discussion with Drs. C. W. Struck and W. H. Fonger of RCA Laboratories, Princeton, N.J., in which she was informed about their most interesting work entitled, "Unified Model of the Temperature Quenching of Narrow Line and Broad Band Emission." In this work, the overlap integrals between the ground and excited states are calculated through the Manneback recursion formulas. We hope to extend their approach in the future for calculation of c–c diagram in glasses.

References

1. S. Parke and R. S. Webb, *J. Phys. Chem. Solids* **34**, 85 (1973).
2. R. Reisfeld and S. Morag, *Appl. Phys. Letters* **21**, 57 (1972).
3. R. Reisfeld and N. Lieblich, *J. Non-Crystalline Solids* **12**, 207 (1973).
4. R. Reisfeld and L. Boehm, *J. Non-Crystalline Solids* **16**, 83 (1974).
5. S. Parke and R. S. Webb, *J. Phys. Ser. D. Appl. Phys.* **4**, 825 (1971).
6. G. Blasse and A. Bril, *J. Chem. Phys.* **47**, 1920 (1967).
7. M. J. Weber and R. R. Monchamp, *J. Appl. Phys.* **44**, 5495 (1973).
8. R. Reisfeld and Y. Eckstein, *J. Solid State Chem.* **5**, 174 (1972).

9. R. REISFELD, R. A. VELAPOLDI, AND L. BOEHM, *J. Phys. Chem.* **76**, 1293 (1972).
10. C. R. GOLDSCHMIDT, G. STEIN, AND E. WURZBERG, to appear.
11. K. PATEK, *in* "Glass Lasers" (J. G. Edwards, Ed.), p. 72, Butterworth, London (1970).
12. A. FUKUDA, *Sci. of Light* **13**, 64 (1964).
13. B. JACQUIER, G. BOULON, G. SALLAVUARD, AND F. GAUME-MAHN, *J. Solid State Chem.* **4**, 374 (1972).
14. M. F. TRINKLER AND I. K. PLYAVIN, *Phys. Status Solidi* **11**, 277 (1965).
15. T. S. DAVIS, E. R. KREIDLER, J. A. PARODI, AND T. F. SOULES, *J. Luminescence* **4**, 48 (1971).
16. R. REISFELD, *J. Res. of Nat. Bur. Stand. A.* **76**, 443 (1972).
17. R. ENGLMAN AND B. BARNETT, *J. Luminescence* **3**, 55 (1970).
18. D. CURIE (Ed.), Luminescence in Crystals", p. 49, Methuen, London (1963).